NOTATION

ℓ, length of liquid column in capillary at time t; r, capillary radius; L, capillary length; η, liquid dynamic viscosity coefficient; σ, liquid surface tension coefficient; ρ, liquid density; θ, static wetting angle; g, acceleration of gravity; α, angle of inclination of the capillary to the horizontal; τ, empirical proportionality coefficient; z, v, τ_0, τ_1, a, ℓ^*, new variables; k_1, k_2, roots of characteristic quadratic equation.

LITERATURE CITED

1. A. P. Porkhaev, Kolloid. Zh., 11, No. 5, 346-353 (1949).
2. V. I. Kolesnichenko, "Heat and mass transport processes in thermovacuum purification of fillers from titanium sponges," Preprint IMSS UNTs Akad. Nauk SSSR, No. 235 [in Russian], Sverdlovsk (1983).
3. A. V. Kuz'mich, P. A. Novikov, and V. I. Novikova, Inzh. Fiz. Zh., 50, No. 2, 294-299 (1986).

INFLUENCE OF A POSITIVE PRESSURE GRADIENT ON THE CHARACTERISTICS OF A TURBULENT BOUNDARY LAYER

V. V. Zyabrikov

UDC 532.526

Based on a systematic analysis of present day experimental data published in the literature, a modified Prandtl–Clauser turbulence model is presented which makes it possible to take into account the effect of a positive pressure gradient on the average characteristics of a turbulent boundary layer.

Determination of the characteristics of a turbulent boundary layer subject to the action of a positive pressure gradient constitutes a difficult problem from the experimental point of view. Proceedings of the Stanford Conference of 1980/81 (see [1]) show that there is as yet no full set of published experimental data that exhausts this problem (especially as far as the region before separation is concerned). According to the valid opinion of the authors of [2, 3], the difficulty in making an experimental study of the region close to the point where the turbulent boundary layer separates is associated with the emergence of short-duration reverse flows at a significant distance from the "stationary" separation point and with the need for using measuring instruments sensitive to the direction of the rate of flow. Although the first paper on this theme appeared in 1968 (see [2]), it is only recently that sufficiently detailed results of systematic measurements have been published [4-6] that justify modification of the Prandtl-Clauser model of turbulence. The present research was conducted under the guidance of L. G. Loitsyanskii.

Distribution of Longitudinal Velocity and Frictional Stress in the Interior Region of a Turbulent Boundary Layer. By the interior region of a turbulent boundary layer we mean that portion of it in which the turbulent viscosity increases with increasing distance from the wall. In contrast to the exterior region the interior region depends weakly on the prehistory of the flow and possesses a relative autonomy: The characteristics of this region can be regarded as functions only of the parameters of pressure gradient $p_* = (\nu/\rho)(dp/dx)/v_*^3$ and convective acceleration $g_* = \nu(dv_*/dx)v_*^2$ [7]. The interior region of the turbulent boundary layer with a positive pressure gradient consists of a viscous sublayer, a transitional portion, a logarithmic region, and a half-power law subregion [8]. The problem of determining the damping factor in the transition section was examined in detail in [7-9]. For a positive pressure gradient of arbitrary magnitude the damping factor can be approxi-

M. I. Kalinin Leningrad Polytechnical Institute, Leningrad.

Translated from Inzhenerno-Fizicheskii Zhurnal, Vol. 57, No. 2, pp. 232-239, August, 1988. Original article submitted February 18, 1988.

0022-0841/89/5702-0904$12.50

© 1990 Plenum Publishing Corporation

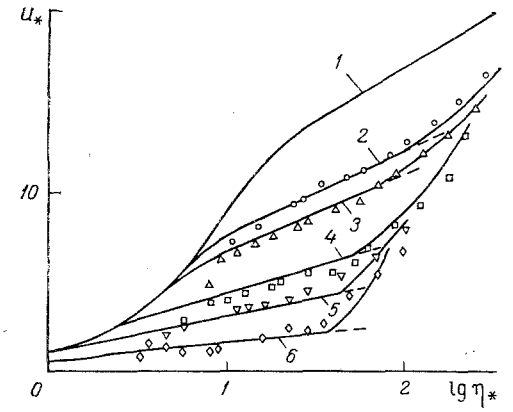

Fig. 1

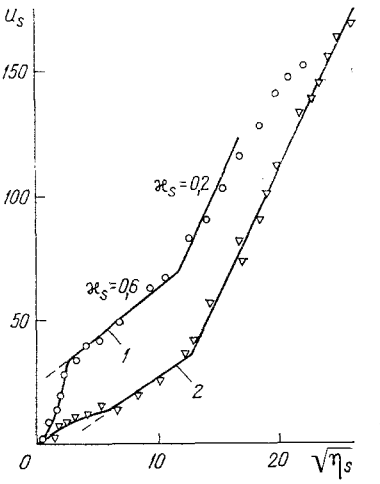

Fig. 2

Fig. 1. Velocity profile in interior region of turbulent boundary layer in wall coordinates: Values of p* for curves 1-6 are 0; 0.021; 0.028; 0.062; 0.105; 0.282. Points plotted are experimental data from [4, 5]; continuous curves represent calculations from relations (1)-(4), (6), (7).

Fig. 2. Turbulent boundary layer velocity profile in stratford coordinates: Values of p_* for curves 1 and 2 are 0.021 and 0.105, respectively. Plotted points are for experimental data from [4, 5]; continuous curves correspond to calculations from relations (1)-(4), (6), and (7); dashed curves correspond to the exterior half-power law.

mated by the following formula, which takes into account the experimental data of [4, 5] and is somewhat different from that given in [7]:

$$D_* = 0{,}0008 \exp(50p_*)(1 + p_*\eta_*)^2\eta_*^2, \quad (\eta_* \leqslant \eta_{*0}),$$
$$D_* = 1, \quad (\eta_* > \eta_{*0}), \tag{1}$$
$$\eta_{*0} = (\sqrt{1 + 4p_*/\sqrt{0{,}0008 \cdot \exp(50p_*)}} - 1)/(2p_*).$$

Here $\eta_* = yv_*/\nu$ is the ordinate of the wall; η_{*0} is the value of this ordinate at which the damping factor D_* becomes equal to one. The longitudinal velocity profile $u_* = u/v_*$ at an arbitrary point of the interior region is given by the expression (see, for example, [7]):

$$u_* = 2\int_0^{\eta_*} \frac{\tau_* d\eta_*}{1 + \sqrt{1 + 4\tau_* l_{p*}^2 D_*}}, \tag{2}$$

where $l_{p*} = l_p v_*/\nu$ is the dimensionless Prandtl mixing path length; $\tau_* = \tau/\tau_W$ is the dimensionless frictional stress. Over its whole extent, starting from the wall and up to the end of the logarithmic portion, the length of the mixing path is given by the Reeves formula [7]:

$$l_{p*} = \varkappa_* \eta_* \sqrt{\tau_*}, \tag{3}$$

while the frictional stress distribution is given by Coles' formula [10]:

$$\tau_* = 1 + p_*\eta_* + g_* I_*(\eta_*), \; I_*(\eta_*) = \int_0^{\eta_*} u_*^2 d\eta_*. \tag{4}$$

With the function $\varkappa_*(p_*)$ known, relations (2)-(4) constitute a closed system of equations for determination of the functions $u_*(\eta_*)$ and $\tau_*(\eta_*)$. This system can be solved iteratively. However, as numerical calculations have shown, if for the first approximation over the whole portion, starting from the wall and up to the end of the logarithmic portion, we take the logarithmic velocity profile

$$u_* = \frac{1}{\varkappa_*} \ln \eta_* + B_*, \tag{5}$$

substituting it into formula (4) and calculating the integral $I_*(\eta_*)$

$$I_*(\eta_*) = \frac{\eta^*}{\varkappa_*^2}[\ln \eta_* + \varkappa_* B_* - 1)^2 + 1], \tag{6}$$

we then immediately obtain a sufficiently exact distribution $\tau_*(\eta_*)$. If we then substitute the function $\tau_*(\eta_*)$ so defined into formula (2) and integrate numerically, we obtain the exact distribution of the longitudinal velocity $u_*(\eta_*)$. In practically all the known experiments in the literature the order of magnitude of the convective acceleration parameter g_* does not exceed 10^{-5} in absolute value, as a result of which continuation of the iterational process changes the resulting distributions at most 1%, and, consequently, the iterations can be discontinued.

The manner in which the coefficients κ_* and B_* in the logarithmic velocity profile (5) depend empirically on the pressure gradient parameter p_* is obtained from experimental data in [4-6], the result being

$$\begin{aligned} \varkappa_* &= \begin{cases} 0{,}4\ (p_* \leqslant 0{,}006), \\ 0{,}36 + 7{,}2p_*\ (p_* > 0{,}006), \end{cases} \\ B_* &= \begin{cases} 5{,}1\ (p_* \leqslant 0{,}006), \\ 0{,}118\,(p_* + 0{,}017)^{-1}\ (p_* > 0{,}006). \end{cases} \end{aligned} \tag{7}$$

The latter expressions combine the law of conservation of the logarithmic velocity profile [11] for small pressure gradients and the law of conservation of the form of logarithmic dependence for large pressure gradients [4-6]. The function $B_*(p_*)$ was used in the derivation of the damping factor (1). The empirical formulas (7) reflect the fact, noted by many authors (see [6, 12, 13]), that there is a lowering of the logarithmic segment on the graph of the velocity profile in comparison with the gradientless boundary layer and a decrease in its angle of inclination to the axis of abscissas to zero at the separation point, where the logarithmic dependence becomes zero [4, 5]. These effects are illustrated in Fig. 1 where we present experimental data from [4, 5] and the results of calculations made in accordance with relations (1)-(4), (6), and (7). As is evident from the figure, starting roughly at $p_* = 0.05$, at the joining point η_{*1} a discontinuity occurs in the derivative $\partial u/\partial y$ due to the emergence of an intermediate zone between the logarithmic region and the half-power law region.

Interior and Exterior Half-Power Laws. The half-power law was introduced by analogy with the logarithmic law on the basis of Prandtl's formula for the turbulent friction stress τ_t and the assumption of a linear variation of τ_t with respect to y, valid in the immediate vicinity of the wall. In stratford variables we have [7]:

$$\eta_S = \frac{y v_S}{\nu}, \quad u_S = \frac{u}{v_S}, \quad \pi_S = \left(\frac{v_*}{v_S}\right)^2, \quad \left(v_S = \sqrt[3]{\frac{\nu\,(dp/dx)}{\rho}}\right) \tag{8}$$

the half-power law has the form [8]:

$$u_S = \frac{2}{\varkappa_S} \sqrt{\eta_S} + B_S. \tag{9}$$

where in a first approximation the coefficient κ_S can be considered to be independent of the stratford pressure gradient parameter π_S:

$$\varkappa_S \cong 0{,}6. \tag{10}$$

The portion on which the half-power law (9), (10) is valid is situated in the interior region above the logarithmic portion. We call this law the interior half-power law. To determine the distribution of friction in the zone where this law applies, we transform the velocity profile coordinates (9), (10) into wall coordinates using the relationships [7]:

$$\eta_S = p_*^{1/3} \eta_*, \quad u_S = p_*^{-1/3} u_*, \quad \pi_S = p_*^{-2/3}. \tag{11}$$

After substituting the resulting profile into formula (4), we obtain

$$I_*(\eta_*) = I_*(\eta_{*1}) + S_*(\eta_*) - S_*(\eta_{*1}),$$
$$S_*(\eta_*) = p_*^{2/3}\eta_*\left(\frac{2}{\varkappa_S^2}\ p_*^{1/3}\eta_* + \frac{8}{3}\ \frac{B_S}{\varkappa_S}\ \sqrt{p_*^{1/3}\eta_* + B_S^2}\right); \tag{12}$$

η_{*1} is the boundary coordinate between the logarithmic portion and the interior half-power law region, being defined by the union of the profiles (5), (7) and (9), (10). Formulas (4) and (12), in totality, constitute an analytical expression for the distribution of friction in the region where the interior half-power law is valid.

The authors of [14] gave a derivation of the half-power law based on a theory of dimensionality and they confirmed the validity of this law using experimental data relating to the exterior region. In [6] experimental confirmation was given of the fact that in the exterior region of the pre-separated boundary layer from $y/\delta = 0.25$ to $y/\delta = 0.7$ the longitudinal velocity varies according to the square root of the transverse coordinate. In the exterior region the turbulent friction stress does not grow linearly. Thus, our concern is with the derivation of a new exterior half-power law for the velocity profile. In Fig. 2, with the aid of experimental data from [4, 5], presented in stratford coordinates, one can observe simultaneously both interior (slope $\varkappa_S = 0.6$) and exterior ($\varkappa_S = 0.2$) half-power laws. As shown by experimental data [15] and the calculations in [8], the exterior half-power law applies in a gradientless turbulent boundary layer; it also holds for a laminar self-similar Falkner–Skan family of velocity distributions.

Coefficients of the exterior half-power law, in contrast to the interior half-power law, are not subject to regularities of the type (10) and depend strongly on specific frictional conditions; therefore they can be called laws only by convention. The simultaneous existence of two half-power laws can even be observed in the first experimental data obtained in this region by Stratford (see, for example, Fig. 2.7 on p. 31 of [16]). Until now, an existing incorporation of the two half-power laws into one is not justified and leads to a large scatter in the experimental values of the coefficients [14].

Modification of Clauser's Formula for Turbulent Viscosity in the Exterior Region of a Turbulent Boundary Layer. The formula most used for the exterior region is Clauser's formula

$$\nu_t = KU\delta^*, \quad \left(\tau_t = \rho\nu_t\ \frac{\partial u}{\partial y}\right). \tag{13}$$

Clauser's empirical constant K represents a dimensionless turbulent viscosity in the exterior region [17] and in a gradientless turbulent boundary layer has the value $K = 0.0168$ [18]. The widely held opinion that this constant value can also be used in the case of a positive pressure gradient proves to be not the case, as was shown in [17]. Theory of dimensionality considerations and the effect of a degeneration of the interior region with approach to the separation point, as described in [17], show that the Clauser constant must be a decreasing function of the pressure gradient parameter in the exterior region: $\beta = (dp/dx)\delta^*/\tau_W$. Diminution of the constant K with an increase in β also follows from the treatment of the experimental data [2] and is in agreement with the empirical formula of Kuhn and Nielsen [19]. In spite of the fact that in [20], in connection with a disregard of short-duration reverse flows and, possibly, errors of numerical differentiation of the velocity profile, the opposite conclusion is made, we can consider the tendency of the constant K to decrease with an increase in the parameter β as established.

The question as to the size of the Clauser constant at the separation point of a turbulent boundary layer is debatable. The authors of [17], relying on the vanishing of the zone adjacent to the wall for generation of turbulent frictional stress, together with degeneration of the interior region, suggest taking the constant K equal to zero in the separated section, which leads to the vanishing of the turbulent viscosity and the frictional stress throughout the separated section. The experimental data in [4] indicate that the turbulent frictional stress not only does not vanish in a separated section but even increases due to an increase in the derivative $\partial u/\partial y$ as this section is approached. An increase in this derivative in the exterior region of the turbulent boundary layer leads to an increase in the generation of turbulent frictional stress in it, which is confirmed by thermo-anemometric measurements [21], and a corresponding compensation in the decrease of wall-adjacent generation of turbulent shear stresses. The latter means that the Clauser constant must assume a small, but nonzero, value, the determination of which is hampered by the impossibility of

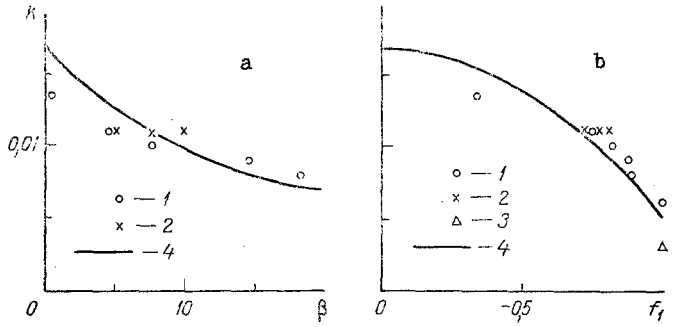

Fig. 3. Dependence of the Clauser constant K on the pressure gradient parameter β (Fig. 3a) and f_1 (Fig. 3b). Points labeled 1, 2, and 3 correspond to experimental data from [4, 5], [6], and [2], respectively. Points labeled 4 correspond to the approximation formulas (14).

reproducing exactly the situation of equilibrium separation. Taking into account the value of K = 0.003, obtained from an analysis of the experimental data in [2], and the value of K = 0.006 resulting from the experimental data in [4], we shall accept for the Clauser constant in the section of separation the following value: K = 0.005. In Fig. 3 we present the functions $K(\beta)$ and $K(f_1)$, and their approximations

$$K = 0{,}005 + 0{,}0118\exp(-0{,}1\beta),$$
$$K = 0{,}0168 - 0{,}0118 f_1^2. \qquad (14)$$

determined experimentally in accordance with [4, 6].

Here $f_1 = (U'\delta^{**}/U)/(c_f/2 - U'\delta^{**}/U) = \beta/(H - \beta)$ is the parameter introduced in [22], which, in comparison with β, has the advantage that it varies within finite limits, from zero in the gradientless section to −1 in the separated section. We remark that the second of formulas (14) approximates the experimental data more precisely than the first.

Profile of the Longitudinal Velocity in the Separated Section of the Turbulent Boundary Layer. On the basis of a comparison of characteristic experimental data and the results of calculations, the authors of [2] came to the following conclusion, at first glance rather paradoxical: In the separated section the laminar and turbulent boundary layer velocity profiles, written in y/δ and u/v coordinates, coincide. In spite of the fundamental value of this conclusion it has not been discussed further in the literature, and the question as to the form of the turbulent velocity profile in the separated section is still an open one. Verification of this important result, which we made on the basis of a comparison of the new experimental data [4, 5] and a calculated self-similar separated profile of the Falkner–Skan family [8], confirmed the coincidence of the laminar and turbulent velocity profiles (see Fig. 4). This coincidence is stipulated by the fact that with approach to the separation point there occurs, in connection with a sharp diminution of thickness of the interior region [17], an ordinate-wise leveling (to what level is immaterial) of the turbulent viscosity profile. We recall the existence of two regions in an arbitrary, non-separated, turbulent boundary layer: an interior region and an exterior region, where the turbulent viscosities in the two regions differ strongly in magnitude, a fact which leads to a characteristic difference in form of the turbulent velocity profiles from the laminar velocity profiles.

Coincidence of the velocity profiles does not mean laminarization of the flow; although the turbulent viscosity in the separated section is roughly 3 times less than in the gradientless section (see the formula in [14]), it is altogether several orders larger than the laminar.

For comparison, Fig. 4 shows the equilibrium velocity profile (dashed curve) calculated using the Sebesi–Smit turbulence model [18], the calculations being carried out according to the method described in [22]. Contradiction of the calculations from the latter model, composed for the gradientless case, with experimental data for the turbulent boundary layer in a separated section arises from exaggeration in the model of the role of the interior region and is a glaring illustration of the need for the modification described in our paper. The proposed improvement in the classical Prandtl–Clauser turbulence model consists

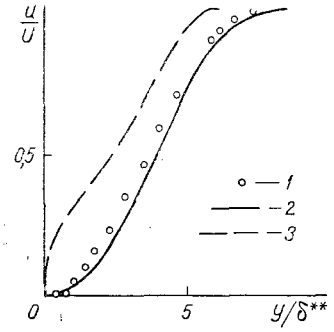

Fig. 4. A comparison of an experimental turbulent velocity profile in a separated section, using data from [4, 5] (points labeled 1), with a laminar separated velocity profile of the Falkner–Skan family [8] (points labeled 2) (H = 4.0). Also shown is a turbulent separated velocity profile calculated using the Sebesi–Smit model from [18, 22] (H = 2.4) (points labeled 3).

in the use of prepared formulas for the velocity profile in the interior region and in the necessity of integrating the differential equation of the turbulent boundary layer with a modified Clauser formula for viscosity in the exterior region. This arrangement corresponds to the well-known property of greater sensitivity of the exterior region to a change in the flow parameters and it substantially eases the numerical integration of the boundary layer equation, making it unnecessary to introduce an integration step varying with respect to the ordinate. Formulas for the velocity profile and frictional stress, in the interior region which properly reflect the influence of a positive pressure gradient, can be used in the capacity of functions near the wall and in more involved turbulence models.

NOTATION

p_*, pressure gradient in interior region; ν, kinematic viscosity coefficient; ρ, density; p, pressure; x, longitudinal coordinate; v_*, dynamic velocity; D_*, damping factor; η, dimensionless transverse coordinate; u, longitudinal velocity; ℓ, displacement pathlength; τ, frictional stress; η_{*0}, value of coordinate η_* at boundary between transition section and logarithmic region; g_*, convective acceleration parameter; I_*, integral in Coles' formula; κ_* and B_*, logarithmic law coefficients; κ_S and B_S, half-power law coefficients; π_S, pressure gradient parameter in interior region expressed in stratford variables; v_S, stratford velocity scale; S_*, function used in calculating integral I_* in half-power law region; δ, physical thickness of boundary layer; ν_t and τ_t, turbulent viscosity and frictional stress, respectively; U, velocity at exterior boundary of boundary layer; δ^*, displacement thickness; K, Clauser constant; β, pressure gradient parameter in exterior region; τ_W, frictional stress at the wall; f_1, normalized pressure gradient parameter in exterior region; δ^{**}, momentum loss thickness; c_f, friction coefficient; subscripts * and S refer, respectively, to Prandtl (law of the wall) and stratford variables; a prime refers to differentiation with respect to variable x; H is the ratio of displacement thickness to momentum loss thickness.

LITERATURE CITED

1. S. J. Kline, G. M. Lilley, and B. J. Cantwell, Proceedings of the 1980/81 AFOSR-HTTM Stanford Conference on Complex Turbulent Flow, Vols. 1-3, Dept. of Mech. Eng., Stanford Univ., Stanford, CA (1981).
2. V. A. Sandborn and C. Y. Liu, J. Fluid Mech., 32, Part 2, 293-304 (1968).
3. C. C. Kutateladze, O. N. Kashinskii, and V. A. Mukhin, Gradient and Separated Flows [in Russian], Novosibirsk (1976), pp. 8-48.
4. R. L. Simpson, Y. Chew, and B. G. Shivarprasad, J. Fluid Mech., 113, 23-51 (1981).
5. R. L. Simpson, Trans. ASME, J. Fluid Eng., 103, No. 4, 520-533 (1981).
6. E. M. Khabakhpasheva and G. I. Efimenko, Structure of Forced and Thermogravitational Flows [in Russian], Novosibirsk (1983), pp. 5-31.
7. V. V. Zyabrikov and L. G. Loitsyanskii, Izv. Akad. Nauk SSSR, Mekh. Zhidk. Gaza, No. 5, 46-53 (1987).
8. L. G. Loitsyanskii, Mechanics of Fluids and Gases [in Russian], Moscow (1987).
9. L. G. Loitsyanskii, Inzh.-Fiz. Zh., 45, No. 6, 924-932 (1983).
10. D. Coles, Boundary Layer and Heat Transfer Problems [Russian translation], Moscow–Leningrad (1960), pp. 138-147.
11. H. Ludwig and W. Tillman, Ing. Archiv., No. 17, 288-299 (1949).
12. G. I. Efimenko and E. M. Khabakhpasheva, Gradient and Separated Flows [in Russian], Novosibirsk (1976), pp. 49-69.
13. V. K. Lyakhov, M. I. Deveterikova, Yu. F. Ukrainskii, and S. Ya. Grabarnik, "On failure of the 'wall law' in flows with positive pressure gradient," Moscow (1982). Deposited in VINITI 4/29/82, No. 2124.

14. B. Ya. Kader and A. M. Yaglom, "Effect of roughness and longitudinal pressure gradient on turbulent boundary layers," VINITI. Mekh. Zhidk. Gaza, Itogi Nauki Tekh., No. 18, 3-111 (1984).
15. Proc. of 1968 Conf. on Turbulent Boundary Layer, AFOSR, Stanford Univ., Thermosciences Div., Dept. of Mech. Eng., Vol. 2, Stanford, CA (1969).
16. K. K. Fedyaevskii, A. S. Ginevskii, and A. V. Kolesnikov, Calculation of Turbulent Boundary Layer of an Incompressible Fluid [in Russian], Leningrad (1973).
17. Yu. V. Lapin and M. Kh. Strelets, Teplofiz. Vys. Temp., 23, No. 3, 522-529 (1985).
18. T. Sebesi, A. Smit, and G. Mosinskis, Rocket Technology and Astronautics [Russian translation], 8, No. 11, 66-76 (1970).
19. G. D. Kuhn and J. N. Nielsen, "Prediction of turbulent separated boundary layers," AIAA Paper No. 663 (1973).
20. M. J. Nituch, N. Sjolander, and M. R. Head, Aeron. Quart., 29, No. 3, 207-225 (1978).
21. A. I. Leont'ev, and E. V. Shishov, Turbulent Flows Adjacent to a Wall [in Russian], Novosibirsk (1984), 105-111.
22. V. V. Zyabrikov, Zh. Prikl. Mekh. Tekh. Fiz., No. 5, 74-77 (1982).

ELEMENTARY THEORY OF PSEUDO-TURBULENCE IN FINELY-DISPERSED SUSPENSIONS

Yu. A. Buevich and A. M. Isaev

UDC 532.545

Relations are obtained to characterize the standard deviations of fluctuation velocity and the self-diffusion coefficients of the phase in flows of suspensions of small particles.

Suspended particles and fluid moles are brought into small-scale pulsative (pseudo-turbulent) motion even in flows of suspenions which are macroscopically uniform, and this motion has a significant effect on the distribution of the phases in the flows and the effective heat- and mass-transfer coefficients. Energy for the pulsations is supplied by the work done by the carrier flow against fluctuations in the concentration of the suspension. The forces acting on individual particles differ from the local mean value, which leads to acceleration of the particles. As they accelerate, the particles entrain adjacent moles of fluid [1, 2].

The theory of pseudo-turbulent motion is based on representation of the fluctuations of the concentration, pressure, and velocity of the particles and the fluid in the form of steady-state random functions. These functions are analyzed using the equations of fluctuational gasdynamics, which are in turn obtained directly from the averaged equations of mass and momentum conservation for the phases of a suspension [3, 4]. The calculations prove to be very cumbersome in this case. In addition, there is a logical contradiction; the linear scale of the unknowns in the averaged equations is assumed to be much greater than the dimensions of the particles in the suspension, but these equations are in essence being used to describe fluctuations with a scale on the order of these dimensions. Here, we attempt to circumvent this problem and at the same time simplify the calculations.

We will examine a flow of a monodisperse suspension of fine spherical particles. The local values of the mean phase velocities and the pressure and concentration of the particles are determined from the solution of the hydrodynamic equations of the suspension and, in the analysis of pseudo-turbulence, are assumed to be known quantities independent of the coordinates and time. The latter assumption is justified by the fact that the temporal and linear scales of these means must be significantly greater than the corresponding scales for the pulsations.

A. M. Gorky Ural State University. Translated from Inzhenerno-Fizicheskii Zhurnal, Vol. 57, No. 2, pp. 239-246, August, 1989. Original article submitted March 23, 1988.

 0022-0841/89/5702-0910$12.50 © 1990 Plenum Publishing Corporation